Design and development of innovative FBG-based fiber optic sensors for aerospace applications

Design and development of innovative FBG-based fiber optic sensors for aerospace applications

Design and development of innovative FBG-based fiber optic sensors for aerospace applications

M D L Dalla Vedova, P C Berri, P Maggiore and G Quattrocchi

Dept. of Mechanical and Aerospace Engineering, Politecnico di Torino, Torino, Italy

E-mail: matteo.dallavedova@polito.it

Abstract. In recent years aeronautical systems are becoming increasingly complex, as they are often required to perform various functions. New intelligent systems are required capable of self-monitoring their operation parameters, able to estimate their health status, and possibly perform diagnostic or prognostic functions. For these purposes, these systems frequently need to acquire several different signal types; although it is sometimes possible to implement virtual sensor techniques, it is usually necessary to implement dedicated sensing hardware. On the other hand, the installation of the required sensors can, however, significantly increase the complexity, the weight, the costs and the failure rate of the entire system. To overcome these drawbacks, new types of optical sensors, minimally invasive for measuring the system parameters and having a high spatial resolution and a minimum added complexity are now available. Fiber Bragg Gratings (FBGs) sensors are suitable for measuring various technical parameters in static and dynamic mode and meet all these requirements. In aerospace, they can replace several traditional sensors, both in structural monitoring and in other system applications, including mechatronic systems diagnostics and prognostics. This work reports the results of our experimental research aimed at evaluating and validating different FBG installation solutions such as deformation, bending, vibration, and temperature sensors. These were compared with numerical simulations results and measurements performed with traditional strain gauges and accelerometers.

1. Introduction

In recent years, optical fibers adoption in the aerospace sector has steadily increased. They offer several desirable characteristics compared to classical electrical transmission lines (i.e. copper cables), including wider bandwidth, EMI insensibility, lower latency and lightness, particularly pronounced over long transmission distances. Furthermore, optical fibers are strongly resistant to aggressive environments, including extreme temperatures and corrosive chemicals. On the other hand, the major setbacks of optical fibers adoption is the geometrical constraints (i.e. minimum fibers curvature radii), the necessity of an electro-optical interface, whose cost is still high given the low production volumes due to relatively niche applications, and the high sensitivity to mechanical shocks and damages.

Besides the classical passive applications, i.e. transmission lines, optical fibers can be used as active components by leveraging light signals properties like intensity, phase shift, polarization and spectral bandwidth, enabling the construction of minimally invasive transducers [1-7]. In this work, Fiber Braggs Gratings (FBGs) will be analyzed [8]; such sensors consist in a periodic modulation of the refractive index of the fiber, generally obtained by UV photoetching.

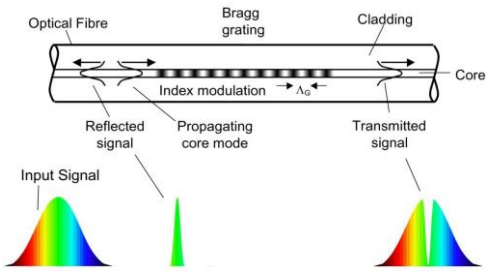

Figure 1. Schematic diagram of an FBG inside a single-mode optical fiber [1].

The process produces regions with higher refractive index compared to the fiber; the effect is the reflection of a sub-nanometer wavelength band (Bragg wavelength), given by this linear relation:

$$\lambda_B = 2n\Lambda_G \tag{1}$$

where λ_B is the Bragg wavelength, n is the refractive index of the fiber, and Λ_G is the pitch of the grating (figure 1). A consequence of the relationship between reflected wavelength and etched gratings pitch is its ability to measure mechanical strain, either direct or temperature-induced. In particular:

$$\Delta\lambda_B = K_\varepsilon \Delta\varepsilon + K_T \Delta T \tag{2}$$

where K_ε and K_T are the strain and temperature coefficients [9-11]. This equation shows a coupling between mechanical and thermal effects; thus, proper thermal compensation logic must be implemented if only strains are of interest. Given the extremely high sensitivity of FBGs, an ideal application would be in fault detection and estimation of remaining useful life of mechatronic systems, e.g. as very accurate strain sensors for electromechanical and electrohydrostatic servomechanisms. The application would allow the sensing of external loads acting on the elements, so that such values could be leveraged in software to modify and optimize the dynamical response of the system considering the current estimated damage level, while at the same time reducing wear propagation rate. Furthermore, FBGs sensors could be used as minimally invasive temperature sensing elements, detecting localized overheatings which often are indicators of incipient faults in electrical motors and solenoid valves. Additional PHM (Prognostics and Health Management) applications are in vibration analysis of rotating machinery (e.g. mechanical transmissions, turbomachinery) and in composite structures health monitoring, where high spatial resolution (i.e. strain measures) can be leveraged to detect localized damages like delaminations [12]. In this work, the authors present first results of an experimental campaign aimed at evaluating and validating different installation solutions suitable for using FBGs as deformation, vibration and temperature sensors. These are compared with numerical simulations results and measurements performed with traditional strain gauges and accelerometers.

2. Static axial strain tests

2.1 Test bench assembly

As reported in [8], the authors' research started with experiments aiming to define the proper bonding techniques and performing static tests in different environmental conditions. To this purpose, a test bench has been developed to perform strain and thermal analyses. The critical factors to control are vibrations and fiber locking systems. Tests and results, widely described in [13], allowed finding the best locking solution to performing high precision strain test. Test samples are, as previously described, small lengths of optical fibers containing the sensing element (FBG). Fibers are clamped at both ends and a preload is imposed via a micrometric actuator, with a linear resolution in the order of 10 μm. Fibers free length l_0 is not constant but is kept around 10-20 cm, allowing a strain resolution of 10^{-5}. At one end of each fiber an optical connector is installed, allowing the coupling with the optical interrogator; the interrogator sends a light impulse spanning a variable wavelengths band and detects the wavelengths reflected; the wavelength shift allows the measurement of strain or temperature.

On the same fiber several FBGs can be mounted, making sure to use elements with different base wavelength. Using multiple sensors on a single optical line can greatly reduce system complexity and increases compactness and lightness. Regarding vibrations, two main sources were identified: the first originated by street traffic and people walking by near the bench, and the second originated by temperature gradients induced by the air conditioning. To mitigate these problems, an optical table is used; furthermore, sorbothane dampers [14, 15] with a characteristic time of 2 seconds are placed between the table and the breadboard. Regarding air circulation, a plexiglass enclosure was used to isolate the bench from air currents and a software low-pass filter was also implemented.

2.2 Fiber bonding techniques

Using the FBGs as strain sensors impose the bonding of the optical fiber to the structure that must be measured, using a connection as rigid as possible. Connection rigidity is paramount since a non-rigid connection does not accurately follow the element deformation thus increasing measuring error. However, fibers mechanical fragility must be accounted; the locking system needs to be designed in such a way that avoids excessive mechanical stresses. Locking systems based on mechanical clamping have been firstly considered by authors [8] (figure 2), either using a layer of soft material (e.g. expanded neoprene or 1,3-butadiene) to spread the load on the fibers and protect the sensing zone. Subsequently, gluing the fiber to a 3D-printed PLA holding plate has been tested using several commercially available epoxy resins or cyanoacrylate glues (figure 3). Each clamping methodology offers advantages, but also presents disadvantages. Mechanical clamping, for example, allows the reutilization of every component, while gluing creates a permanent joint between fiber and holding plate. Mechanical locking allows a maximum strain value before slip starts to occur, while epoxy does not present this behavior since the bonding is much stronger. However, the stiffness is reduced and thus the response time, which is also affected by viscoelastic phenomena. Furthermore, temperature, humidity, epoxy mixing and application uniformity have great effects on the behavior of glued joints.

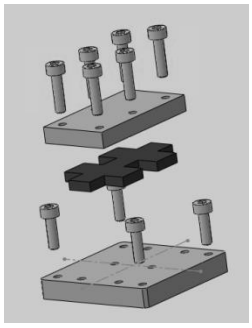

Figure 2. Mechanical clamping locking system [8].

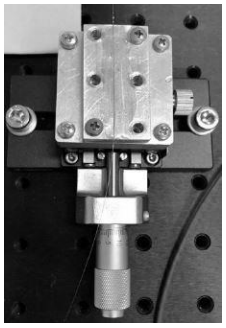

Figure 3. Example of epoxy resin gluing locking system.

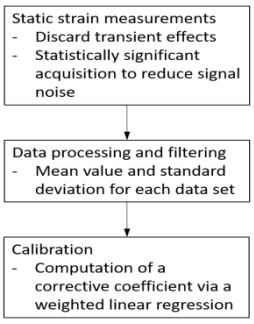

Figure 4. Measurement and data processing procedure.

2.3 Fiber bonding techniques

To obtain a preliminary validation of the techniques described above, a simplified statistical approach has been used. The procedure shown in figure 4, should be summarized with the following steps.

Static strain measurements: in this phase, FBGs are set to a predetermined strain ad kept in such condition for an amount of time long enough to log a sufficient number of samples using the interrogator. Several strain conditions are analyzed, waiting enough time between two different measure conditions in order to achieve mechanical equilibrium.

Data processing and filtering: logged data are then imported in MATLAB for processing. Mean value and standard deviation are calculated, in order to filter zero-mean high frequency noise.

Sensor calibration: using a linear regression on the filtered points, weighted with the standard deviation, the correlation between strain and wavelength is analyzed, for each bonding method. The ratio between the theoretical slope $K_{\varepsilon\,th}$ (Eqn. 2) and the experimental slope, $K_{\varepsilon\,ex}$ is the corrective coefficient K, used for sensor calibration.

Raw data from the analyzer have been used in the analysis, in order to have better control on the data. Filtering and elaboration integrated in the interrogator software suite has been disabled, and all processing is done in a MATLAB script. Differences between theoretical and empirical values on the strain-wavelength curve can be pointed to elastic effects such and slippage of the different systems. In order to reduce uncertainty and to calibrate the test bench, repeatability tests have been performed for each locking system and an average corrective coefficient for each locking system has been calculated.

2.4 Results of static axial strain tests

The comparison of different installation techniques has shown that mechanical locking with a rubber layer is worse to glue locking systems. In fact, especially in high strain conditions (5000 με or higher), slipping can occur between the optical fiber and the rubber layer (figure 5).The exact value of strain to produce a slipping depends on the tightening pressure of the clamping; however, an excessive pressure may result in permanent damage to the rubber and optical fiber. On the other hand, bonding with glue provides better performance to the sensor up to high strain values. Since the glue layer accounts for a significant fraction of the total displacement (even in the order of 10%), the compensation of glue elasticity cannot be neglected during data postprocessing. This discrepancy is highlighted by the comparison between measured and imposed displacement in figure 6. The actual strain is determined applying to the raw sensor reading a correction, previously determined through a calibration process

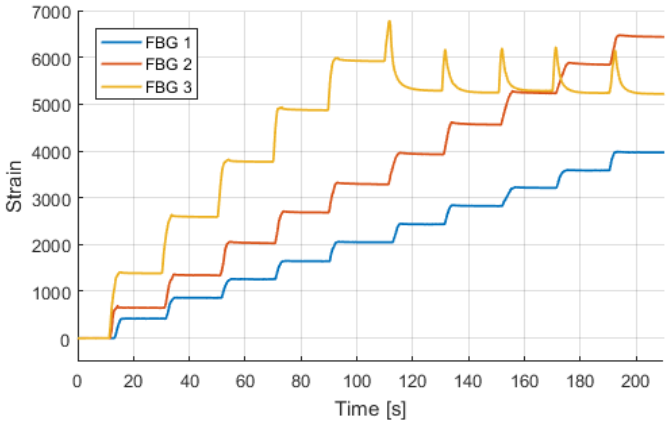

Figure 5. Comparison between rubber clamping and gluing with cyanoacrylate and epoxy resin.

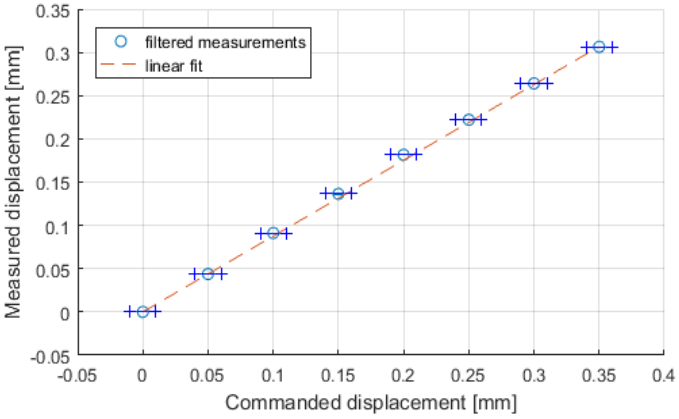

Figure 6. Imposed and measured displacements values (filtered) and related linear fit.

As previously stated, repeatability tests have been performed to assess eventual hysteresis or viscous shear phenomena for the different locking techniques. Tests were performed by repeatedly straining and unloading the sensor [8]. Considering glued fibers, no significant hysteresis has been noted; after load value is set back to null, the FBGs return to center wavelength even after several load cycles. Mechanical clamping, however, express a different behavior: a small displacement induces local sliding of the fiber on the rubber sheet, thus slightly loosening the fixture, i.e. preload is reduced after load is ceased. The reduction in preload is related to a shift in the reflected central wavelength. Furthermore, cyclic sliding damages the rubber layer, given the very high contact pressures, degrading the stability, repeatability, and duration of the joint.

Locking technique	Fiber lengths [mm]	Applied Strain [$\mu\varepsilon$]	Corrective coeff. K	Dispersion
1,3-Butadiene	228.94	4000	1.2135	0.064
Soft expanded neoprene	228.94	4000	1.0769	0.021
Araldite epoxy resin	228.94	2000	1.0012	0.0013
Araldite epoxy resin	151.16	3000	1.0212	0.0045
Araldite epoxy resin	53.59	6000	1.1248	0.0132

Table 1. Performance comparison of different FBG locking techniques [8]

Hysteresis and macroscopic slippage occurring at high strains influence the corrective coefficient K; furthermore, sensor linearity is affected: the fit loses accuracy for high strain values, thus producing more significant measures dispersion. Corrective coefficients K for several test campaigns using different locking techniques are summarized in Table 1, including relevant data such as fiber lengths and displacements imposed. It should be noted that the best performances, expressed in terms of bonding stiffness, durability, and repeatability, have been achieved using Araldite epoxy resin, featuring the lowest values of both correction (i.e. corrective coefficient K) and dispersion.

3. Static tests on beams subject to bending

In the previous chapter, the authors evaluated several techniques to ensure a reliable and sufficiently rigid fixing of the optical fiber on the structure or component that must be sensorized by FBGs. However, to test the applicability and performance of optical sensors based on FBG in real applications (structural, systems engineering, mechatronics, etc.), it is necessary to devise ad hoc procedures that allow you to simulate the actual operating conditions satisfactorily. In detail, in this chapter, the authors investigated the performance of optical sensors applied to structures subject to bending stresses (which, for example, could simulate the stresses acting on wing spars or fuselage structure). Besides, the experimental bench (shown in figure 7) tested two different fiber bonding techniques in the same experiment, to verify the effect that gluing produces on the accuracy and sensitivity of the FBGs. The first is obtained by continuous gluing of a fiber equipped with FBG, and the second is realized by punctual gluing, aiming to achieve a uniform deformation in the whole FBG.

The experimental measurements thus obtained were then validated by comparison with a finite element simulation performed with Nastran-Patran and with the data provided by traditional resistive strain gauges installed in correspondence with FBGs. It should be noted that the simple structure considered would have allowed a more straightforward numerical solution using the Euler-Bernoulli beam theory. However, the authors preferred a 2D finite element solution to take into account local deformations (e.g. due to interaction with the support structure or the load actuator), which can influence the measurements.

3.1 Fiber bonding techniques

Figure 1 represents the proposed experimental setup. The test sample is either an aluminum beam or a composite spar, clamped at one end, and loaded by imposing a displacement with a micrometric linear actuator at the other end. A fiber equipped with three FBGs is glued to the beam, and provides strain measurements. Each Bragg is coupled with two strain gauges to validate the measurements. Numerous tests were performed, comparing different gluing techniques. The method providing the best compromise between flexibility and control over the thickness of the glue layer consisted in applying pressure to the glue through a soft layer. Additionally, we compared the performances of a continuous gluing and a point gluing. The continuous gluing provides better protection to the fiber, as it is completely incorporated into the glue layer, while point gluing generates a more uniform deformation over the entire length of the Bragg, so as to minimize the wavelength dispersion.

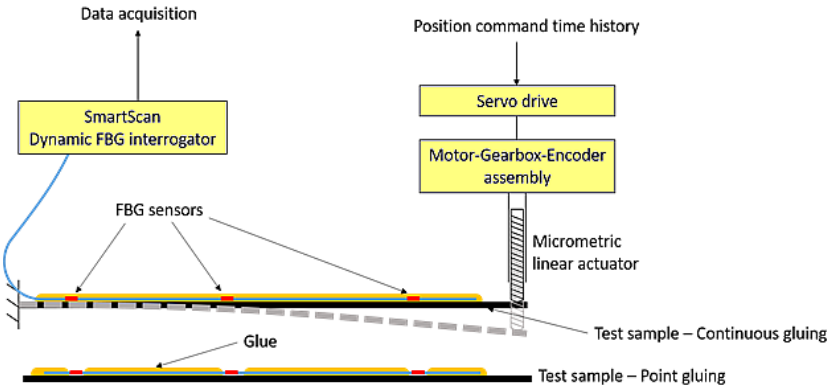

Figure 7. Proposed experimental setup for static bending test.

3.2 Static bending test: results and discussion

Figure 8 shows the result of one of the various measures carried out, expressed in terms of deformation versus displacement. The dashed curve is obtained through a simulation of finite Nastran-Patran elements, while the two solid lines indicate an acceptable range of measurement. In fact, since the thickness of the glue layer is not negligible with respect to the total thickness of the beam, it cannot be assumed that the sensor is positioned precisely on the surface of the beam. The continuous line curves correspond, through Navier's equation, to the deformation experienced by a sensor positioned exactly on the surface of the beam (lower curve) or floating on the glue layer (upper curve) a, as shown in the cross-section of figure 8 (detail in the graph at the bottom right).

Experimental tests that compared punctual and continuous fiber bonding methods produced substantially the same results. That is, we find a slightly higher dispersion of the results in the case of continuous gluing (due to the fact that the deformation is not constant along the entire FBG), but it has been observed that this behavior has a negligible effect on the accuracy of the measurement.

In figure 9, the measurement provided by the single FBG is compared with the average of the two strain gauges placed next to the fiber. It can be seen that the Bragg tends to slightly overestimate the tension (probably due to the thickness of the glue, which slightly increases the distance of the fiber from the neutral axis of the beam). However, its measurement is much less sensitive to signal noise and therefore requires fewer filters. It can be experimentally observed that, when the test sample is maintained with a constant deformation, the measurement provided by the Bragg is almost stationary.

At the same time, the strain gauges (influenced by electromagnetic noise) require more signal conditioning. However, we can reasonably assume that the main uncertainty that afflicts this configuration of the Bragg grating sensors is primarily attributable to the unknown thickness of the glue layer. It must be noted that the depth of this layer of glue is difficult to control during installation, especially on structures of complex shape.

However, the FBGs installation on a real structural component will be less sensitive to this effect since the characteristic dimensions of the structure (and therefore the related distances from the neutral axis of the beam) will almost certainly be orders of magnitude higher than the glue layer thickness. The results obtained all fall within the expected range and show satisfactory correspondence with the experimental validation data (collected through the strain gauges) and simulated data (calculated using a digital twin implemented in Nastran-Patran). Furthermore, it has been verified that continuous gluing produces substantially the same behavior as point gluing. Hence, continuous gluing should be preferred in field applications, as it provides greater strength and protection to the fiber, without significantly affecting the measurements.

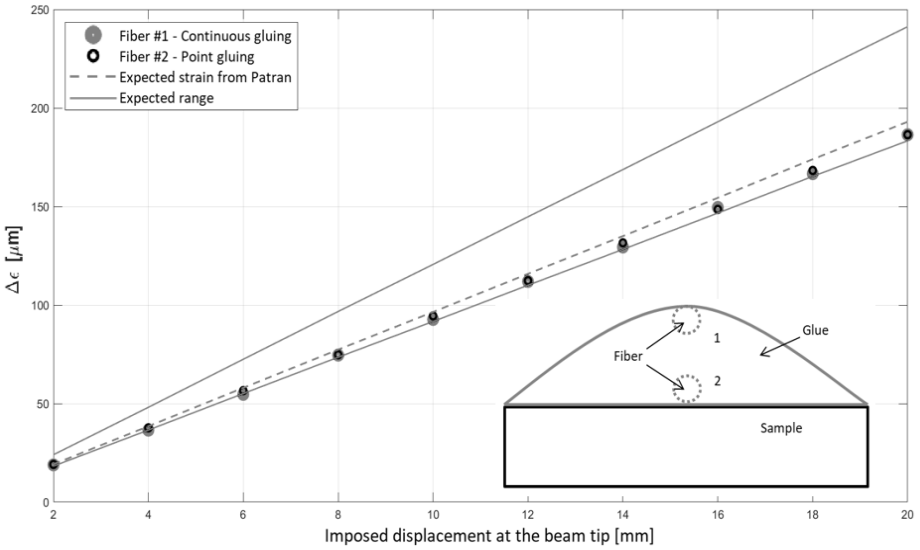

Figure 8. Bragg sensors applied to bending test: comparison between FBG and FEM.

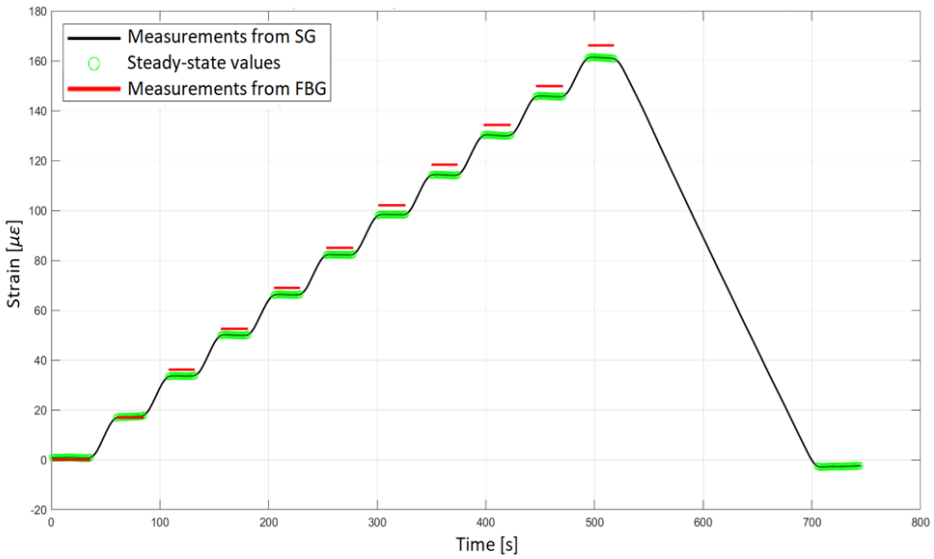

Figure 9. Bragg sensors applied to bending test: FBG vs traditional strain gauges (SG).

4. Conclusions

FBG-based sensors have been evaluated to provide different measurements with a more robust and less invasive installation than traditional technologies. For future space missions, these sensors can be used to control multiple operating parameters of the spacecraft, from launch stresses to operating temperatures, to vibrations caused by the aging of mechanical equipment (e.g. reaction wheels, actuators, robotic arms, etc.). The authors have performed numerous tests, aimed at testing the performance and accuracy of these sensors in different operating scenarios and having to acquire different heterogeneous physical quantities. The results obtained so far have been very encouraging and have shown that the technology considered is now mature for use in aerospace applications. Sensors based on Bragg grating allow high precision measurements with minimally invasive installations and with acceptable operating costs.

Acknowledgements

This work was supported by the Photonext interdepartmental center at Politecnico di Torino. The authors wish to thank the LINKS laboratory for their invaluable assistance to the experimental activities presented in this paper.

References

[1] Mihailov S J 2012 Fiber Bragg grating sensors for harsh environments *Sensors* **12(2)** 1898–1918
[2] Mihailov S J, Grobnic D, Hnatovsky C, Walker R B, Lu P, Coulas D and Ding, H 2017 Extreme Environment Sensing Using Femtosecond Laser-Inscribed Fiber Bragg Gratings *MDPI Sensors* **17(12)** 2909
[3] Habel J, Boilard T, Frenière J S, Trépanier F and Bernier M 2017 Femtosecond FBG written through the coating for sensing applications *MDPI Sensors* **17(11)**, 2519
[4] Grobnic D, Mihailov S, Smelser C W and Ding H 2004 Sapphire Fiber Bragg Grating Sensor Made Using Femtosecond Laser Radiation for Ultrahigh Temperature Applications *IEEE Photonics Technology Letters* **16(11)**, 2505–2507
[5] Santos J L and Farahi F 2018 *Handbook of Optical Sensors* CRC Press
[6] Ahuja D and Parande D 2012 Optical sensors and their applications *J. Sci. Res. Rev.* **1(5)**, 60–8
[7] Giurgiuntiu V 2016 Structural health monitoring of aerospace composites *Fiber-Optic Sensors*
[8] Berri P C, Dalla Vedova M D L, Maggiore P and Scolpito T 2019 Feasibility study of FBG based sensors for prognostics in aerospace applications *Journal of Physics: Conference Series* **1249**, 012015
[9] Kersey A D 1996 A review of recent developments in fiber optic sensor technology *Optical Fiber Technology* 291–317
[10] Tanaka N, Okabe Y, Takeda N 2003 Temperature-compensated strain measurement using fiber Bragg gratings sensors embedded in composite laminates *Smart Mat. & Struct.* 12(6) 940–6
[11] Wenyuan W, Yongqin Y, Youfu G, Xuejin L. 2015 Measurements of thermo-optic coefficient of standard single mode fiber in large temperature range *Proc. Int. Conf. Optical Instr. and Tech.: Optical Sensors and applications (Beijing)* **9620**
[12] Mainini L and Willcox K E 2017 Data to decisions: real-time structural assessment from sparse measurements affected by uncertainty *Computers & Structures* **182** 296–312
[13] Berri P C, Dalla Vedova M D L, Maggiore P and Secci C 2020 Fiber Bragg gratings for prognostics in space applications: a thermo-mechanical characterization of minimally invasive sensing techniques *Proc. 1st Aerospace Europe Conference AEC 2020 (Bordeaux)*
[14] Kasap S 2013 *Optoelectronics and Photonics: Principles and Practices* Pearson Education Ltd.
[15] Yamane M and Asahara Y 2000 *Glasses for photonics* Cambridge University Press